ROYAL SOCIETY OF CHEMISTRY

Water-soluble Ir(III) complexes of deprotonated N-methylbipyridinium ligands: fluorine-free blue emitters†

Benjamin J. Coe,*[a] Madeleine Helliwell,[a] Sergio Sánchez,[a] Martyn K. Peers[b] and Nigel S. Scrutton[b]

New blue or blue-green emitting iridium complexes have been synthesised with cyclometalating ligands derived from the 1-methyl-3-(2′-pyridyl)pyridinium cation. Efficient luminescence is observed in MeCN or aqueous solutions, with a large range of lifetimes in the µs region and relatively high quantum yields.
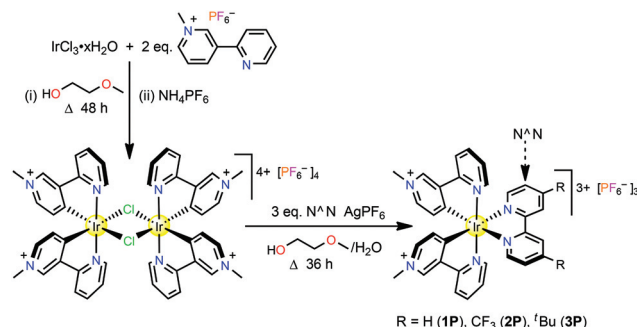
The creation of bright and stable blue emitting compounds is a major challenge in the development of light-emitting electrochemical cells and organic light-emitting diodes (OLEDs).[1,2] Iridium complexes have been investigated extensively due to their widely tunable and efficient luminescence.[2–12] A common structural type is $[Ir^{III}(C\wedge N)_2(N\wedge N)]^+$, where C^N is a cyclometalating ligand like deprotonated 2-phenylpyridine, and N^N is an α-diimine. A popular strategy to blue-shift the emission is to derivatise C^N with electron-withdrawing groups (often –F or –CF$_3$) and/or place electron donors on N^N. Avoiding the use of fluorine is desirable to maximise the stability of the complexes in devices, and from an environmental perspective. Hence, we present an alternative approach, creating new fluorine-free Ir^{III} luminophores by using 1-methyl-3-(2′-pyridyl)pyridinium to generate C^N. The quaternised nitrogen opposite the cyclometalating carbon is key to blue-shifting the emission.

Ir^{III} complexes of C^N ligands derived from pyridinium species are extremely scarce.[13] Notably, these known complexes are not suitable for luminescence, but were prepared in the context of catalytic studies. Complexes with quaternary N units as part of N^N have been reported, but these groups are generally not strongly coupled electronically to the Ir^{III} centre.[14–17] Remote ammonium groups have been attached to C^N[18] or acetylacetonate[19] ancillary ligands. Using Ir^{III}

complexes in bio-sensing/imaging[20] is often restricted by poor water solubility,[21] so increased positive charge is beneficial. Given this context and our general interest in photoactive complexes with quaternised pyridinium moieties,[22] we targeted unusual Ir^{III} species combining attractive emission and solubility properties.

The new complexes 1–3 were synthesised by a standard approach, i.e. cleaving a cyclometalated chloride-bridged dimer with a N^N ligand (Scheme 1). The PF$_6^-$ and Cl$^-$ salts were characterised by ^{1}H NMR spectroscopy, electrospray mass spectrometry and elemental analyses (see ESI†). In addition, single-crystal X-ray structures have been solved for 1P·2MeCN and 3P·3Me$_2$CO (Tables S1 and S3, Fig. S1 and S2, ESI†). As expected, both complexes exhibit pseudooctahedral coordination at Ir, with the pyridyl rings of the C^N ligands in a trans geometry (Fig. 1). Their chemical structures bear some resemblance to the widely studied complexes of N-heterocyclic carbenes derived from imidazolium species, although such complexes are typically neutral or only +1 charged.[23–26]

UV–vis absorption spectroscopic data are shown in Table 1. These spectra are almost unaffected by changing the counter-anions and solvent. They are dominated by intense bands at λ < 320 nm (Fig. S3 and S4, ESI†), assigned to π → π* and high

[a]School of Chemistry, The University of Manchester, Oxford Road, Manchester M13 9PL, UK. E-mail: b.coe@manchester.ac.uk
[b]Manchester Institute of Biotechnology, Faculty of Life Sciences, The University of Manchester, 131 Princess Street, Manchester M1 7DN, UK
†Electronic supplementary information (ESI) available: Details of synthetic, characterisation and theoretical studies. CCDC 1407686 and 1407687. For ESI and crystallographic data in CIF or other electronic format see DOI: 10.1039/c5dt02591e
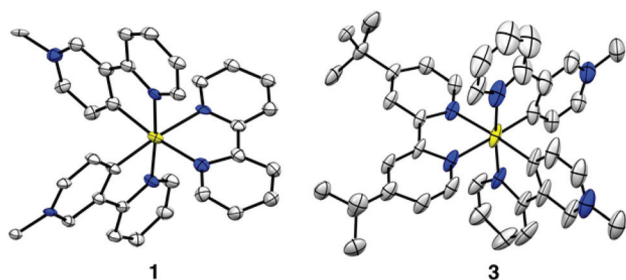
Scheme 1 Synthesis of the complex salts 1P–3P; their chloride counterparts 1C–3C were prepared by treating purified 1P–3P with [^{n}Bu$_4$N]Cl in acetone.

Fig. 1 Representations of the molecular structures of the complex cations in **1P**·2MeCN and **3P**·3Me$_2$CO, with the PF$_6^-$ anions, solvent molecules and H atoms removed for clarity (50% probability ellipsoids).

energy metal-to-ligand charge-transfer (MLCT) transitions, involving both the C^N and N^N ligands. Weaker bands ($\lambda_{max} \approx 350$–356 nm) are observed also. Cyclic voltammograms of **1P**–**3P** in MeCN (Fig. S5, Table S2, ESI†) show an irreversible oxidation, formally assigned to a Ir$^{IV/III}$ couple. The reductive region includes multiple irreversible processes, and a sharp return peak is observed for **1P** and **3P**, indicating adsorption onto the electrode surface.

Excitation at 315–400 nm in deoxygenated and oxygenated MeCN or aqueous solutions leads to bright blue (**1** and **3**) or blue-green (**2**) luminescence (Table 1). The spectra show significant fine structure, indicating primarily ligand-centred emission. As for the absorption spectra, changing the counter-anion and solvent has only slight effects, and the excitation profiles remain constant in all cases while monitoring at all the emission maxima. The spectra are very similar for R = H or ^{t}Bu (λ_{em} = 468–474 nm), but shifted significantly to lower energy when R = CF$_3$ (λ_{em} = 494). The fact that replacing H with ^{t}Bu has little effect while –CF$_3$ groups give a red-shift suggests that the character of the emitting state varies. The almost identical spectra of **1** and **3** (Fig. 2) indicate mainly ^{3}LC emission involving C^N with little ^{3}MLCT contribution. However, the red-shift for **2** suggests that the emission is associated with N^N. The quantum yields ϕ are not affected significantly by the counter-anions under deoxygenated conditions, but are substantially enhanced when R = CF$_3$ or ^{t}Bu ($\phi \approx 42$–45%) as opposed to H ($\phi \approx 24$–27%). In oxygenated conditions, **2** shows the largest ϕ values. All complexes have
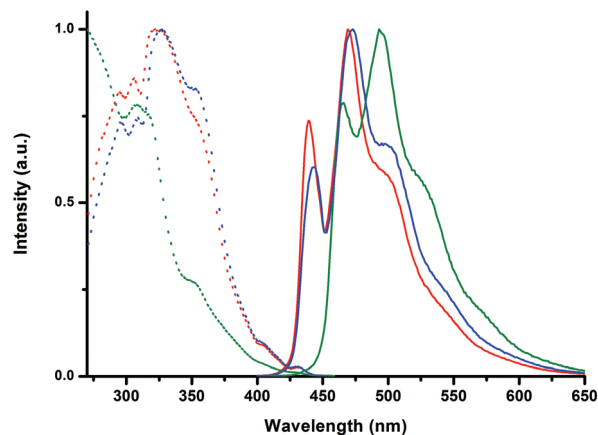

Fig. 2 Emission spectra of **1P** (blue), **2P** (green) and **3P** (red) with excitation at 350 nm in MeCN.
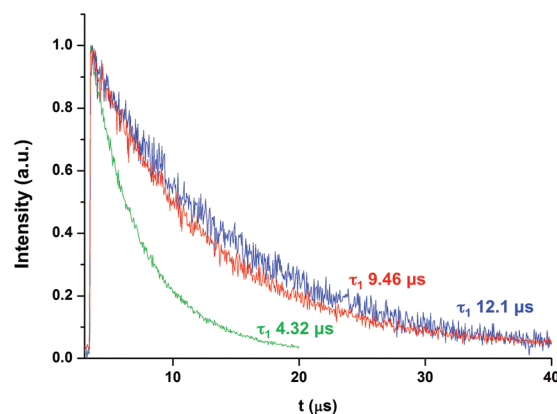

Fig. 3 Emission decay traces in water of **1C** (blue), **2C** (green) and **3C** (red) following 375 nm excitation with a ps pulsed diode laser.

emission lifetimes τ in the μs region, covering a large range of values (*ca.* 1–12 μs), with monoexponential decay kinetics. **1C** and **3C** show relatively long τ values in water, considerably longer than for **2C** (Fig. 3).

Table 1 Absorption and emission data at 298 K in solutions *ca.* 1.0 × 10^{-5}–2.0 × 10^{-4} M. Luminescence data measured in the presence (ox) or absence (deox) of oxygen

Complex salt	Absorption, λ_{max}/nm ($\varepsilon/10^3$ M^{-1} cm^{-1})	Emission, λ/nm	τ^c/μs		ϕ^c (%)	
			deox	ox	deox	ox
1P[a]	237 (54.3), 255sh (48.5), 302 (25.9), 313 (24.5), 352sh (5.3)	444, 474$_{max}$, 504, 548	3.5	1.2	24	4.7
1C[b]	237 (48.3), 255sh (42.4), 302 (22.8), 312 (21.8), 353sh (4.8)	442, 470$_{max}$, 504, 547	12.1	3.9	27	9.7
2P[a]	236 (47.4), 257 (43.2), 308 (21.6), 316 (20.9), 350sh (5.4)	466, 494$_{max}$, 525, 574	3.8	1.5	43	16
2C[b]	237 (52.7), 259 (52.1), 308 (25.2), 317 (24.3), 350sh (5.8)	462, 494$_{max}$, 529, 575	4.3	2.6	42	24
3P[a]	236 (51.8), 259sh (44.9), 299 (23.9), 311 (23.2), 356sh (4.5)	440, 470$_{max}$, 502, 546	3.8	1.2	43	11
3C[b]	237 (58.0), 260 (49.9), 300 (25.4), 312 (25.9), 355sh (5.5)	440, 468$_{max}$, 500, 547	9.5	2.9	45	14

[a] In MeCN. [b] In water. [c] Estimated experimental errors ±10%.

The observed blue emissions from the fluorine-free complexes **1** and **3** are remarkable since, as mentioned above, decorating the C^N ligands with F or fluorinated groups is a common strategy to blue-shift the emission of this type of complex. The influence of the pyridinium fragment located *para* to the cyclometalating carbon is clearly shown by comparing the emission properties of **3P** (λ_{max} = 470 nm, ϕ_{deox} = 43%, τ_{deox} = 3.8 ms) with other reported complexes [Ir^{III}(C^N)$_2${4,4'-(^{t}Bu)$_2$bpy}]$^+$. When using the heavily fluorinated cyclometalating ligand derived from 2-(2,4-difluorophenyl)-5-trifluoromethylpyridine, the emission in MeCN (λ_{max} = 470 nm, ϕ_{deox} = 68%, τ_{deox} = 2.3 ms) is similar to that of **3P**.[27] On the other hand, when C^N is deprotonated 2-phenylpyridine, the emission in MeCN is red-shifted strongly (λ_{max} = 581 nm) with a lower ϕ_{deox} (24%) and shorter τ_{deox} (0.56 ms).[28]

The singlet ground (S$_0$) and lowest triplet excited (T$_1$) states of **1–3** were optimised by using density functional theory (DFT) (Fig. S6–S9, Tables S3–S8, ESI†). The calculated ground-state structures for **1** and **3** reproduce well the X-ray crystallographic ones. The LUMO is located on the C^N (69–90%) and N^N (6–27%) ligands. The HOMO is located at the Ir atom (50–55%) and the C^N ligands (40–46%), and is essentially invariant. Such relatively high C^N contributions are consistent with the irreversible oxidations observed by cyclic voltammetry (see above). The spectra simulated by time-dependent DFT agree relatively well with those measured. The weak low energy bands are due to a single transition for **1** and **3**, a mixture of HOMO → LUMO and HOMO → LUMO+1 (347 nm, **1**) or HOMO → LUMO (348 nm, **3**). For **2**, transitions occur at 342 nm (HOMO → LUMO+1) and 336 nm (HOMO−2 → LUMO), with the latter being *ca.* 5-fold more intense. These results indicate ^{1}MLCT character with ^{1}ML'CT and also ^{1}LL'CT for **1** and **2** (L = C^N; L' = N^N).

The T$_1$ geometries resemble the S$_0$ ones, except that **1** and **3** now have unequal Ir–C and (chemically equivalent) Ir–N distances, while in **2**, these pairs of distances are equal. The calculated emission energies (Table 2) follow the experimental trend (**1** ≈ **3** > **2**). The spin densities for the T$_1$ state (Fig. 4) show mainly ^{3}LC involving one C^N ligand with some ^{3}MLCT contribution for **1** and **3**. In contrast, for **2**, the spin density is located on N^N largely, indicating that the emission has ^{3}L'C character with some ^{3}ML'CT. Therefore, on excitation from the C^N/Ir-centred HOMO−2 to the C^N-centred LUMO (336 nm transition) 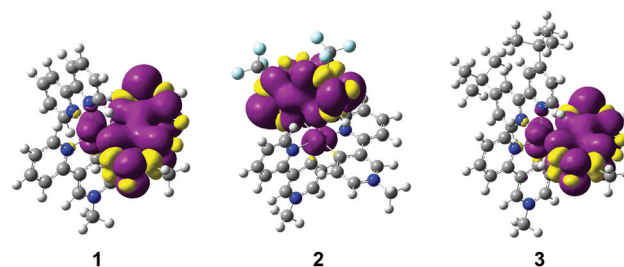in **2**, there is efficient inter-ligand energy transfer to the emitting ^{3}L'C excited state of N^N. Such energy transfer is expected if the ^{3}L'C state lies below the ^{3}MLCT.[29] In **2**, the presence of the electron-withdrawing –CF$_3$ groups stabilises the π* orbitals of the N^N ligand, lowering the energy of the ^{3}L'C state.

To conclude, using 1-methyl-3-(2'-pyridyl)pyridinium to generate C^N affords new water-soluble Ir^{III} complexes. Their excited-state and emissive behaviour can be switched between two types by modifying N^N. The bright blue emission in MeCN and water of the fluorine-free complexes **1** and **3** suggests potential uses in highly efficient OLEDs or bioimaging. The tunability of the emission properties is shown, not only by the emission maxima, but also in the range of quantum yields (*ca.* 5–45%) and lifetimes, from quite short (*ca.* 1 μs) to relatively long (*ca.* 12 μs). Much further scope exists for modifying properties, for example by using groups other than methyl on the quaternised N atom.

Fig. 4 M06/Def2-QZVP/SVP-calculated spin density plots for the T$_1$ state of complexes **1–3**.

Notes and references

1 X.-L. Yang, X.-B. Xu and G.-J. Zhou, *J. Mater. Chem. C*, 2015, **3**, 913–944.

2 Y. Chi and P.-T. Chou, *Chem. Soc. Rev.*, 2010, **39**, 638–655.

3 M. S. Lowry and S. Bernhard, *Chem. – Eur. J.*, 2006, **12**, 7970–7977.

4 J. A. G. Williams, A. J. Wilkinson and V. L. Whittle, *Dalton Trans.*, 2008, 2081–2099.

5 M. Mydlak, C. Bizzarri, D. Hartmann, W. Sarfert, G. Schmid and L. De Cola, *Adv. Funct. Mater.*, 2010, **20**, 1812–1820.

6 C.-H. Yang, M. Mauro, F. Polo, S. Watanabe, I. Muenster, R. Fröhlich and L. De Cola, *Chem. Mater.*, 2012, **24**, 3684–3695.

7 P. Brulatti, R. J. Gildea, J. A. K. Howard, V. Fattori, M. Cocchi and J. A. G. Williams, *Inorg. Chem.*, 2012, **51**, 3813–3826.

Table 2 Predicted and measured emission data in MeCN

Complex	$E_{0,0}$/eV (λ/nm)	E_{AE}/eV (λ/nm)	λ_{max}/nm (exp)
1	2.91 (426)	2.46 (504)	474
2	2.76 (450)	2.28 (544)	494
3	2.91 (426)	2.47 (503)	470

$E_{0,0}$ calculated by using the DFT-optimised geometries for T$_1$ and S$_0$. E_{AE} calculated by using the DFT-optimised T$_1$ geometry for both states (adiabatic electronic emission).

8 N. Mohd Ali, V. L. MacLeod, P. Jennison, I. V. Sazanovich, C. A. Hunter, J. A. Weinstein and M. D. Ward, *Dalton Trans.*, 2012, **41**, 2408–2419.

9 N. M. Shavaleev, F. Monti, R. D. Costa, R. Scopelliti, H. J. Bolink, E. Ortí, G. Accorsi, N. Armaroli, E. Baranoff, M. Grätzel and M. K. Nazeeruddin, *Inorg. Chem.*, 2012, **51**, 2263–2271.

10 E. Baggaley, D.-K. Cao, D. Sykes, S. W. Botchway, J. A. Weinstein and M. D. Ward, *Chem. – Eur. J.*, 2014, **20**, 8898–8903.

11 N. Darmawan, C.-H. Yang, M. Mauro, R. Fröhlich, L. De Cola, C.-H. Chang, Z.-J. Wu and C.-W. Tai, *J. Mater. Chem. C*, 2014, **2**, 2569–2582.

12 J.-B. Kim, S.-H. Han, K. Yang, S.-K. Kwon, J.-J. Kim and Y.-H. Kim, *Chem. Commun.*, 2015, **51**, 58–61.

13 G. Song, Y. Zhang, Y. Su, W. Deng, K. Han and X. Li, *Organometallics*, 2008, **27**, 6193–6201.

14 E. Zysman-Colman, J. D. Slinker, J. B. Parker, G. G. Malliaras and S. Bernhard, *Chem. Mater.*, 2008, **20**, 388–396.

15 Y. Ma, S.-J. Liu, H.-R. Yang, Y.-Q. Wu, C.-J. Yang, X.-M. Liu, Q. Zhao, H.-Z. Wu, J.-C. Liang, F.-Y. Li and W. Huang, *J. Mater. Chem.*, 2011, **21**, 18974–18982.

16 F. Cucinotta, A. Guenet, C. Bizzarri, W. Mróz, C. Botta, B. Milián-Medina, J. Gierschner and L. De Cola, *ChemPlusChem*, 2014, **79**, 45–57.

17 H. Ahmad, A. Wragg, W. Cullen, C. Wombwell, A. J. H. M. Meijer and J. A. Thomas, *Chem. – Eur. J.*, 2014, **20**, 3089–3096.

18 P. Sun, X. Lu, Q. Fan, Z. Zhang, W. Song, B. Li, L. Huang, J. Peng and W. Huang, *Macromolecules*, 2011, **44**, 8763–8770.

19 H.-F. Shi, H.-B. Sun, H.-R. Yang, S.-J. Liu, G. Jenkins, W. Feng, F.-Y. Li, Q. Zhao, B. Liu and W. Huang, *Adv. Funct. Mater.*, 2013, **23**, 3268–3276.

20 S.-J. Liu, H. Liang, K. Y. Zhang, Q. Zhao, X.-B. Zhou, W.-J. Xu and W. Huang, *Chem. Commun.*, 2015, **51**, 7943–7946.

21 S. Stimpson, D. R. Jenkinson, A. Sadler, M. Latham, A. Wragg, A. J. H. M. Meijer and J. A. Thomas, *Angew. Chem., Int. Ed.*, 2015, **54**, 3000–3003.

22 B. J. Coe, *Coord. Chem. Rev.*, 2013, **257**, 1438–1458 and references therein.

23 C.-F. Chang, Y.-M. Cheng, Y. Chi, Y.-C. Chiu, C.-C. Lin, G.-H. Lee, P.-T. Chou, C.-C. Chen, C.-H. Chang and C.-C. Wu, *Angew. Chem., Int. Ed.*, 2008, **47**, 4542–4545.

24 H. Sasabe, J.-i. Takamatsu, T. Motoyama, S. Watanabe, G. Wagenblast, N. Langer, O. Molt, E. Fuchs, C. Lennartz and J. Kido, *Adv. Mater.*, 2010, **22**, 5003–5007.

25 S. B. Meier, W. Sarfert, J. M. Junquera-Hernández, M. Delgado, D. Tordera, E. Ortí, H. J. Bolink, F. Kessler, R. Scopelliti, M. Grätzel, M. K. Nazeeruddin and E. Baranoff, *J. Mater. Chem. C*, 2013, **1**, 58–68.

26 F. Monti, M. G. I. La Placa, N. Armaroli, R. Scopelliti, M. Grätzel, M. K. Nazeeruddin and F. Kessler, *Inorg. Chem.*, 2015, **54**, 3031–3042.

27 M. S. Lowry, J. I. Goldsmith, J. D. Slinker, R. Rohl, R. A. Pascal Jr., G. G. Malliaras and S. Bernhard, *Chem. Mater.*, 2005, **17**, 5712–5719.

28 J. D. Slinker, A. A. Gorodetsky, M. S. Lowry, J.-J. Wang, S. Parker, R. Rohl, S. Bernhard and G. G. Malliaras, *J. Am. Chem. Soc.*, 2004, **126**, 2763–2767.

29 Y. You and S. Y. Park, *J. Am. Chem. Soc.*, 2005, **127**, 12438–12439.